

Studying the Influence of Slip Effects on MHD Casson Nanofluid Flow over a Permeable Stretching Sheet with Variable Wall Thickness.

K saikumar, Department of ECE, Koneru Lakshmaiah Education Foundation, India-522302,

saikumarkayam4@ieee.org

SK ahammad , Department of ECE, Koneru Lakshmaiah Education Foundation, India-522302,

Abstract

An investigation was conducted to examine the influence of slip mechanisms on the magnetohydrodynamic (MHD) flow of Casson nanofluid over a permeable stretching sheet. Furthermore, we documented various flow characteristics, including thermal radiation, variable wall thickness, and chemical reaction. By employing the similarity transformation approach, we transformed the partial differential equations governing the flow into nonlinear ordinary equations. Subsequently, we employed the Homotopy Analysis Method (HAM), a well-known semi-analytical technique, to solve these equations, yielding power series solutions for nonlinear differential equations. To demonstrate the effects of velocity, temperature, and concentration profiles, we conducted a parametric study using tables and diagrams. Our numerical results closely align with previous research findings in a comparative sense. Notably, higher values of the velocity slip parameter led to an augmentation in fluid velocity, whereas increased thermal slip values were associated with a reduction in temperature distribution.

Introduction

The foundation of the nanofluid concept lies in the dispersion of nano-sized particles within a liquid medium. There exist potential advantages in incorporating nanoparticles (NPs) into base fluids. Notably, NPs possess a high surface-to-volume ratio, which enhances their capabilities. When NPs are integrated into other compounds, their durability, stability, resistance to chemicals and heat, as well as susceptibility to light and other radiation, are improved. Incorporating particles with higher thermal conductivity into fluids addresses the low thermal conductivity observed in industrial fluids, benefiting sectors such as pharmaceuticals, medicine, food, and cosmetics. For instance, nanorobots introduced into the bloodstream contribute to healing and recovery mechanisms. Nanotechnology holds significant potential in the development of hybrid technologies, thereby enhancing aspects of healthcare, refining processes, and providing cost-effective assets. The concept of nanofluids was introduced by Choi [1]. Bahiraei et al. [2] investigated the influence of diverse rib configurations and nanoparticle shapes on outcomes. Prasanna kumara [3] explored the impact of a stronger ferromagnetic interaction factor on flow, heat transfer, and the coefficient of local skin friction. Sreedevi et al. [4] discussed the effects of slip conditions and chemical reactions on the mass and heat transport properties of magnetohydrodynamic hybrid nanofluids. Ali Khan et al. [5]

elucidated the consequences of multiple slips on buoyant nanofluid flow over an axisymmetric magnetohydrodynamic (MHD) stretching sheet, considering factors like radiation and chemical influences. Furthermore, Sharma et al. [6] delved into the influence of thermal radiation on Maxwell nanofluid behaviour. Subsequent to these studies, numerous scholars [7–9] formulated diverse mathematical models to further explore this fascinating field.

Current literature reveals a scarcity of research findings concerning the magnetohydrodynamic (MHD) flow behavior of Casson nanofluid influenced by velocity power index, variable wall thickness, and slip effects over a porous stretching sheet [10-12]. The ongoing study is directed towards addressing this gap by focusing on critical parameters that significantly influence the fluid characteristics of Casson nanofluid at the interface. This article introduces a novel approach by employing the Homotopy Analysis Method (HAM) [13], a numerically efficient technique, to tackle the interconnected nonlinear differential equations governing the system. It is worth emphasizing that the selection of precise values for the auxiliary constraints can lead to enhanced accuracy in the obtained results.

Mathematical formulation

In this segment, we analyse a consistent two-dimensional laminar flow of Casson nano liquid under the influence of magnetohydrodynamics (MHD) [14-15]. The flow occurs across a stretched plate with varying wall thickness, while accounting for slip constraints and the momentum flow power index within a permeable medium. The schematic diagram of the boundary layer in the context of a porous medium is depicted in Figure 1.

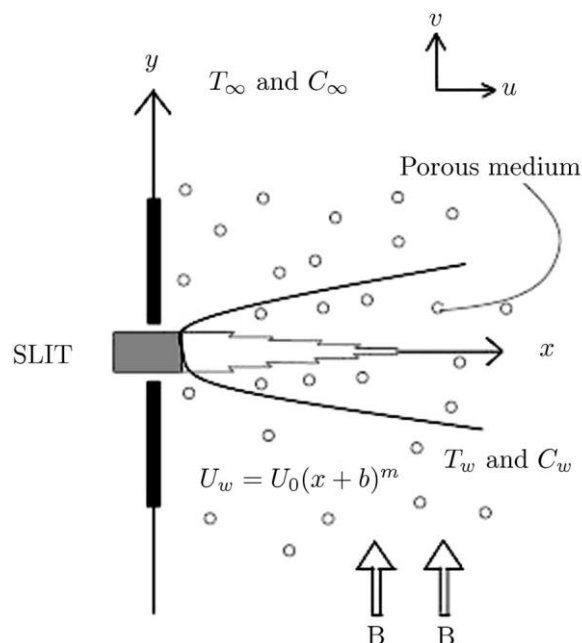


Fig.1.Physical model

The equations regulating the flow can be expressed as follows under these assumptions:

$$\frac{\partial u}{\partial x} + \frac{\partial v}{\partial y} = 0, \quad (1)$$

$$u \frac{\partial u}{\partial x} + v \frac{\partial u}{\partial y} = \nu \left(1 + \frac{1}{\beta}\right) \frac{\partial^2 u}{\partial y^2} - \frac{\sigma B^2(x)}{\rho} u - \frac{\nu}{k_1} u, \quad (2)$$

$$u \frac{\partial T}{\partial x} + v \frac{\partial T}{\partial y} = \frac{1}{(\rho c_p)_f} \frac{\partial}{\partial y} \left(\kappa \frac{\partial T}{\partial y} \right) - \frac{1}{(\rho c_p)_f} \frac{\partial q_r}{\partial y} + \frac{(\rho c_p)_p}{(\rho c_p)_f} \left[D_B \frac{\partial C}{\partial y} \frac{\partial T}{\partial y} + \frac{D_T}{T_\infty} \left(\frac{\partial T}{\partial y} \right)^2 \right], \quad (3)$$

$$u \frac{\partial C}{\partial x} + v \frac{\partial C}{\partial y} = D_B \frac{\partial^2 C}{\partial y^2} + \frac{D_T}{T_\infty} \frac{\partial^2 T}{\partial y^2} - Kr (C - C_\infty), \quad (4)$$

$$\left. \begin{aligned} u &= U_w(x) + \delta_1 \frac{\partial u}{\partial y} = U_0(x+b)^m + \lambda_1 \frac{\partial u}{\partial y}, \quad v = 0, \\ T &= T_w + \lambda_2 \frac{\partial T}{\partial y}, \quad C = C_w + \lambda_3 \frac{\partial C}{\partial y} \end{aligned} \right\} \text{at } y = (x+b_1)^{\frac{1-m}{2}}, \quad (5)$$

$$u = 0, \quad T = T_\infty, \quad C = C_\infty \quad \text{as } y \rightarrow \infty,$$

$$q_r = -\frac{4\sigma^*}{3k^*} \frac{\partial T^4}{\partial y}, \quad (6)$$

$$T^4 = 4T_\infty^4 T - 3T_\infty^4. \quad (7)$$

Then, by Eqs. (6) and (7), we attain

$$\frac{\partial q_r}{\partial y} = -\frac{16\sigma^* T_\infty^3}{3k^*} \frac{\partial^2 T}{\partial y^2}. \quad (8)$$

The similarity variables being considered are

$$\zeta = \sqrt{\frac{U_0(m+1)}{2\nu}} \left(y(x+b)^{\frac{m-1}{2}} - A \right), \quad \psi = \sqrt{\frac{2\nu U_0}{m+1}} (x+b)^{\frac{m+1}{2}} f(\zeta), \quad (9)$$

$$\theta(\zeta) = \frac{T - T_\infty}{T_w - T_\infty}, \quad \varphi(\zeta) = \frac{C - C_\infty}{C_w - C_\infty},$$

$$\left(1 + \frac{1}{\beta}\right) f''' + f f'' - \frac{2m}{m+1} f'^2 - (M+K) f' = 0, \quad (10)$$

$$\left(1 + \frac{4}{3}R\right) \theta'' + \varepsilon \theta'^2 + \text{Pr} f \theta' + \text{Pr} Nb f \varphi' \theta' + \text{Pr} Nt \theta'^2 = 0, \quad (11)$$

$$\varphi'' + Le \text{Pr} f \varphi' + \frac{Nt}{Nb} \theta'' - \gamma Le \text{Pr} \varphi = 0, \quad (12)$$

$$f'(0) = 1 + (\delta_1) f''(0), \quad f(0) = \lambda \left(\frac{1-m}{m+1} \right) f'(0), \quad \theta(0) = 1 + (\delta_2) \theta'(0), \quad (13)$$

$$\varphi(0) = 1 + (\delta_3) \varphi'(0), \quad f'(\infty) = 0, \quad \theta(\infty) = 0, \quad \varphi(\infty) = 0,$$

The modifications highlighted above have resulted to

$$\left. \begin{aligned} Re_x^{1/2} C_f &= \sqrt{\frac{m+1}{2}} \left(\left(1 + \frac{1}{\beta}\right) f''(0) \right), \quad Re_x^{-1/2} Nu_x = - \left(1 + \frac{4}{3}R\right) \sqrt{\frac{m+1}{2}} \theta'(0), \\ Re_x^{-1/2} Sh_x &= - \sqrt{\frac{m+1}{2}} \varphi'(0) \end{aligned} \right\}, \quad (14)$$

where $Re_x = \frac{U_w(x+b)}{\nu}$ stands a local Reynolds number.

$$L_{11} (f_n(\zeta) - \chi_n f_{n-1}(\zeta)) = \hbar_1 Z_n^f(\zeta),$$

$$L_{22} (\theta_n(\zeta) - \chi_n \theta_{n-1}(\zeta)) = \hbar_2 Z_n^\theta(\zeta),$$

$$L_{33} (\varphi_n(\zeta) - \chi_n \varphi_{n-1}(\zeta)) = \hbar_3 Z_n^\varphi(\zeta),$$

Results

Figures 2–4 illustrate the changes in distributions as the Casson constraint parameter β undergoes variation. The flow distributions undergo significant alterations in response to variations in the Casson constraint β . As β increases and plastic dynamic viscosity rises, a corresponding decrease in velocity occurs, accompanied by changes in temperature and concentration profiles.

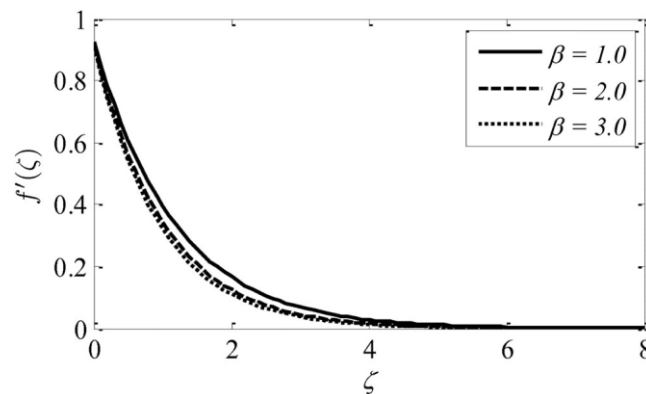


Figure - 2

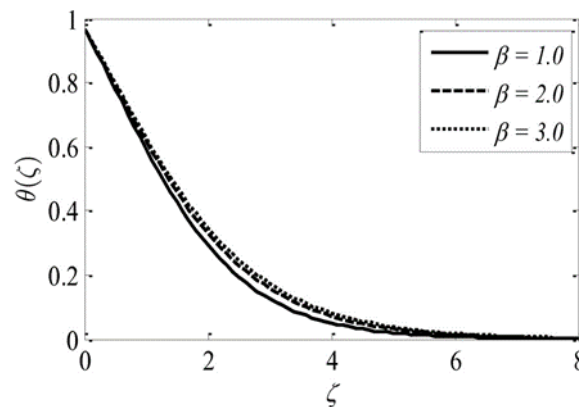


Figure - 3

References

1. Choi, S.U.S., Enhancing Thermal Conductivity of Fluids with Nanoparticles, Procs. of the ASME International Mechanical Engineering Congress and Exposition, San Francisco, CA, USA, 1995, pp. 99–105.
2. Bahiraei, M., Monavari, A., and Moayedi, H., Second Law Assessment of Nanofluid Flow in a Channel Fitted with Conical Ribs for Utilization in Solar Thermal Applications: Effect of Nanoparticle Shape, *Int. J. Heat Mass Transfer*, 2020, vol. 151, p. 119387.
3. Prasannakumara, B.C., Numerical Simulation of Heat Transport in Maxwell Nanofluid Flow over a Stretching Sheet Considering Magnetic Dipole Effect, *Partial Diff. Eqs. Appl. Math.*, 2021, vol. 4, p. 100064.
4. Sreedevi, P., Sudarsan Reddy, P., and Chamkha, A., Heat and Mass Transfer Analysis of Unsteady Hybrid Nanofluid Flow over a Stretching Sheet with Thermal Radiation, *SN Appl. Sci.*, 2020, vol. 2, p. 1222.
5. Ali Khan, S., Nie, Y., and Ali, B., Multiple Slip Effects on Magnetohydrodynamic Axisymmetric Buoyant Nanofluid Flow above a Stretching Sheet with Radiation and Chemical Reaction, *Symmetry*, 2019, vol. 11, no. 9, p. 1171.
6. Sharma, R., Hussian, S.M., Raju, C.S.K., Seth, G.S., and Chamkha, A.J., Study of Graphene Maxwell Nanofluid Flow past a Linearly Stretched Sheet: A Numerical and Statistical Approach, *Chinese J. Phys.*, 2020, vol. 68, pp. 671–683.
7. Ibrahim, S.M., Lorenzini, G., Vijaya Kumar, P., and Raju, C.S.K., Influence of Chemical Reaction and Heat Source on Dissipative MHD Mixed Convection Flow of a Casson Nanofluid over a Nonlinear Permeable Stretching Sheet, *Int. J. Heat Mass Transfer*, 2017, vol. 111, pp. 346–355.
8. Raju, C.S.K., Sanjeevi, P., Raju, M.C., Ibrahim, S.M., Lorenzini, G., and Lorenzini, E., The Flow of Magnetohydrodynamic Maxwell Nanofluid over a Cylinder with Cattaneo–Christov Heat Flux Model, *Cont. Mech. Thermodyn.*, 2017, vol. 29, pp. 1347–1363.
9. Makinde, O.D., Mabood, F., and Ibrahim, S.M., Chemically Reacting on MHD Boundary-Layer Flow of Nanofluids over a Non-Linear Stretching Sheet with Heat Source/Sink and Thermal Radiation, *Thermal Sci.*, 2018, vol. 22, no. 1B, pp. 495–506.
10. Acharya, N., Das, K., and Kundu, P.K., Ramification of Variable Thickness on MHD TiO₂ and Ag Nanofluid Flow over a Slendering Stretching Sheet Using NDM, *Eur. Phys. J. Plus*, 2016, vol. 131, pp. 303–318.
11. Gupta, S., Kumar, D., and Sing, J., Analytical Study for MHD Flow of Williamson Nanofluid with the Effects of Variable Thickness, Nonlinear Thermal Radiation and Improved Fourier's and Fick's Laws, *SN Appl. Sci.*, 2020, vol. 2, pp. 438–449.
12. Shahid, A., Huang, H., Mubashir Bhatti, M., Zhang, L., and Ellahi, R., Numerical Investigation on the Swimming of Gyrotactic Microorganisms in Nanofluids through Porous Medium over a Stretched Surface, *Math.*, 2020, vol. 8, no. 3, pp. 380–397.
13. Sudarsana Reddy, P. and Sreedevi, P., Impact of Chemical Reaction and Double Stratification on Heat and Mass Transfer Characteristics of Nanofluid Flow over Porous Stretching Sheet with Thermal Radiation, *Int. J. Amb. Energy*, 2019, vol. 43, no. 1, pp. 1626–1636.

14. Saikumar, K. (2020). RajeshV. Coronary blockage of artery for Heart diagnosis with DT Artificial Intelligence Algorithm. *Int J Res Pharma Sci*, 11(1), 471-479.
15. Saikumar, K., Rajesh, V. (2020). A novel implementation heart diagnosis system based on random forest machine learning technique *International Journal of Pharmaceutical Research* 12, pp. 3904-3916.